Talanta 232 (2021) 122439

Contents lists available at ScienceDirect

Talanta

journal homepage: www.elsevier.com/locate/talanta

A novel copper (II) binding peptide for a colorimetric biosensor system design

Nuriye Korkmaz [a,*], Changhyun Hwang [a,b], Kim Kristin Kessler [a], Yuliya E. Silina [c], Lisann Müller [a], Jayoung Park [d]

[a] Biosensor Group, Korea Institute of Science and Technology Europe Forschungsgesellschaft MbH, Campus E 7.1, D-66123, Saarbrücken, Germany
[b] Department of Chemical and Biological Engineering, Korea University, Seoul, 02841, South Korea
[c] Institute for Biochemistry, Zentrum für Human und Molekularbiologie (ZHMB), Campus B 2.2, University of Saarland, D-66123, Saarbrücken, Germany
[d] Environmental Safety Group, Korea Institute of Science and Technology Europe Forschungsgesellschaft MbH, Campus E 7.1, D-66123, Saarbrücken, Germany

ARTICLE INFO

Keywords:
Biosensor
Copper
Phage display
Genetic engineering
Filamentous phages

ABSTRACT

Filamentous bacteriophages are viruses infecting only bacteria. In this study, phage display technique was applied to identify highly selective Cu(II) binding peptides. After five rounds of positive screening against Cu(II) and various rounds of negative screenings against competitive metal ions (Al(III), Co(II), Fe(III), Ni(II) and Zn (II)), bacteriophages were enriched. Selective Cu(II) binding of final phages was confirmed by Enzyme Linked Immunosorbent Assay (ELISA), Scanning Electron Microscopy (SEM) and Energy Dispersive X-ray spectroscopy (EDX) analyses. 15 phage plaques were randomly selected and sequenced. Cu-5 peptide (HGFANVA) with the highest frequency of occurrence and the strongest Cu(II) affinity was chosen for further Cu(II) detection and removal tests. Inductively Coupled Plasma-Mass Spectrometry (ICP-MS) confirmed the strong Cu(II) binding potential of engineered viruses. Cu-5 peptides were synthetically synthesized with three Cysteine units at C-terminal and a AuNP-peptide biosensor system was developed based on aggregation behavior of AuNPs upon Cu (II) ion treatment. AuNP-based Cu(II) sensor was selective for Cu(II) and the LOD was 91.15 nM (ca. 5.8×10^{-3} mg/L; $3\sigma/k$, $n = 5$, $R^2 = 0.992$) for the case study which is considerably lower than the WHO's accepted guideline of 1.3 mg/L. This study provides an interdisciplinary approach to apply short peptides as recognition units for biosensor studies which are user friendly, not bulky and cost-effective.

1. Introduction

Heavy metals are metallic elements with molecular weights between 63.5 g/mol and 200.6 g/mol having a specific gravity larger than 5.0 g/cm^3 [1]. Some heavy metals are absolutely essential for living species like iron, zinc, cobalt, copper, nickel, manganese and molybdenum, but at lower concentrations [1]. Toxic effects are seen at higher concentrations due to the accumulation of these ions in living species. Non-essential heavy metals such as cadmium, mercury, chromium, lead and arsenic are extensively utilized in industry and they are classified as hazardous and toxic for human health [2]. Rapid growth of mining, metal processing, energy storage, fertilizer, pesticide and pharma industries resulted in accumulation of toxic heavy metals in the environment. Therefore, trace level detection and removal of heavy metals is crucial [3].

Selective detection of metal ions in complex matrices is not only required for concentration measurements but also for exact identification of the metal species without any interference. Conventional non-electrochemical detection techniques of metal ions include atomic absorption spectroscopy (AAS), atomic fluorescence spectroscopy (AFS) and inductively coupled plasma-mass spectrometry (ICP-MS) [4]. These methods are expensive, time consuming, not portable and require well-educated professionals [5]. Moreover, selectivity is a critical performance criterion for designing sensors. Interference of other analytes present in the sample should be well considered whilst sensor manufacturing and analyses [6].

Biosensors are sensing devices composed of biological recognition elements and pysicochemical detector or transducer units. Due to their simple design, miniaturized size, rapid analysis time and relatively high accuracy, various biosensors have been developed for metal ion detection studies including whole cell biosensors [7] and enzyme-based sensors [8]. For example, bacterial cells have been genetically

* Corresponding author.
E-mail address: n.korkmaz@kist-europe.de (N. Korkmaz).

https://doi.org/10.1016/j.talanta.2021.122439
Received 22 February 2021; Received in revised form 15 April 2021; Accepted 16 April 2021
Available online 23 April 2021

programmed to function as a biosensor [9]. A whole cell biosensor has been developed using *E.coli* cells, which were genetically engineered to express a reporter GFP (green fluorescent protein) encoding gene tagged with an arsenic controllable promoter domain. If there is arsenic in the environment, the promoter is activated resulting in the expression of the reporter protein which can be detected and correlated to the amount of arsenic present in the medium [10]. As an alternative to whole cell biosensors, enzymes metabolizing arsenic could act as biorecognition elements. For instance, arsenite oxidase, which is an enzyme from chemolithoautotroph NT-26 and contains molybdenum as the cofactor, has been applied for As(III) detection [11]. Unfortunately, not every metal ion has a metalloregulatory protein. Therefore, it is necessary to obtain highly specific domains which would selectively recognize the target metal ion. M13 phages are filamentous viruses which can only infect *E. coli* cells (F^+ strains) [12]. M13 viruses were the first time genetically modified by George P. Smith to generate a library of viruses displaying foreign peptides for phage biopanning experiments [13]. Phage display technology employs these libraries of M13 phages to identify target binding peptides after several rounds of selection experiments. Phage selection experiments, in this study, were conducted with Ph.D.-7 phage library solution (NEB GmbH, Germany). According to the manufacturer, the library solution is composed of engineered M13 viruses displaying heptapeptides on their P3 tail coat proteins with a complexity of 10^9 different amino acid sequences which is pretty close to the pre-calculated diversity of 1.28×10^9, which corresponds to all possible amino acid combinations forming a heptapeptide. Until now, specific peptides binding selectively to nanoparticles [14], proteins [15], cancer cells [16] and metal ions like Ni(II) [17], Cd(II) [18], Pb(II) [19], Cr(III) [20] and As(III) [21] have been discovered using the phage display selection technology.

Copper (Cu) is one of the essential elements for all living organisms required for correct functioning and complex formation of respiratory system enzymes called cytochrome oxidases [22]. However, high concentrations of Cu is known to be a carcinogenic due to its strong DNA damaging potential. Moreover, Cu ions can form malondialdehyde after reacting with lipid hydroxyperoxides. Malondialdehyde can inhibit GSH activity through binding which prevents mitosis [4]. Additionally, Cytochrome P450 can be inhibited by Cu(II) ions which weaknesses our defense system against free radicals [23]. Similar to other heavy metal ions, excess amounts of Cu in human body results in ROS (Reactive Oxygen Species) production activating the expression of apoptotic p38 and p53 proteins causing DNA damage and cell death [4].

Therefore, development of cost efficient and simple Cu(II) sensing technologies as an alternative to expensive and sophisticated conventional detection techniques such as AAS, AFS and ICP-MS [4] is important. For example, Chen et al., 2014 [31] developed a colorimetric Cu(II) sensor with AuNPs using a pre-identified Cu(II) binding peptide (SIRKLEYEIEELRLRIG) adapted from a coiled-coil peptide [32]. Moreover, Chang et al., 2017 [33] applied AuNPs as well to detect Cu(II) based on aggregation behavior of AuNPs triggered by electrostatic interactions between ammonium cations of cysteamine molecules, citrate capped AuNPs and Cu(II) ions. Gonzalez et al., 2018 [34] have reported on Histidine (His) included short amino acid sequences and their complex formation with Cu(II) ions. Indeed, His is very well-known for its metal ion complexation properties. As a multi-unit tag (i.e. 6xHis), it is commonly applied for recombinant protein expression studies in order to purify the protein of interest mainly using a Ni-NTA column through Immobilized Metal Ion Affinity Chromatography (IMAC) [35]. His does not only exhibit Cu(II) complexation affinity but also shows a common affinity towards multiple metal ions including Ni(II), Zn(II) and Co(II) [28]. Therefore, in the current study, our approach is to apply the phage display technique in order to identify a highly specific heptapeptide motif against only Cu(II) ions by minimizing the potential binding to other competing metal ions including Ni(II), Zn(II), Co(II) Al(III) and Fe (III).

Selectivity of viruses against Cu(II) ions was further investigated by Enzyme Linked Immunosorbent Assay (ELISA), Scanning Electron Microscopy (SEM) and Energy Dispersive X-ray spectroscopy (EDX) analyses. A microcarrier host system was designed by immobilizing Cu(II) specific virus filaments on cytopore beads which were applied for selective Cu(II) adsorption tests through Inductively Coupled Plasma-Mass Spectrometry (ICP-MS) analyses. Synthetically synthesized Cu(II) specific peptides tagged with Cys units at C-terminal was successfully applied along with 20 nm AuNPs to develop a functional and selective sensor system for Cu(II) ion detection with a LOD of 91.15 nM (3σ/k, $n = 5$, $R^2 = 0.992$) equivalent to ca. 5.8×10^{-3} mg/L which is much lower than the World Health Organization (WHO)'s guideline of 1.3 mg/L [4] implying that this biosensor could be used for on-site detection of Cu(II) ions from complex matrices including environmental samples or body fluids.

2. Materials and methods

2.1. Biopanning for identification of Cu(II) binding phages

Phage selection experiments were conducted with Ph.D.-7 phage library solution (NEB GmbH, Germany). In order to select the viruses which can specifically recognize only Cu(II) ions, it is needed to perform positive and negative screenings as schematically demonstrated in Fig. 1. Negative screening against unloaded NTA beads was conducted as the first step by diluting 100 μL of Ph.D.-7 phage library solution (NEB GmbH, Germany) with 900 μl citrate buffer (pH 4, Acros Organics, Belgium) and mixing with 100 μl of NTA beads (Cube Biotech, Germany) on a rolling drum for 30 min at room temperature. Beads were separated from unbound phages using a 20 μm mesh sized filter (pluriSelect Life Science, Germany). Unbound viruses were further amplified using *E.coli* 2738 cells as suggested by the manufacturer (Ph.D.-7 Phage display peptide library kit, NEB GmbH, Germany).

Amplified virus library solution was used for positive screening against Cu(II) loaded NTA beads like the negative screening but this time the beads were collected on the filter and washed by pipetting at least 10 ml of citrate buffer through the filter. Filter carrying the beads was then transferred onto a 2 ml microfuge tube and the bound phages were eluted using 2.3 ml of EDTA solution (0.5 M, pH 8.0, VWR Chemicals, Germany) after incubating for 10 min while pipetting the solution up and down in every 3 min. The filtrate solution containing the eluted phages was applied to a protein concentrator (Amicon Ultra 100 kDa NMWCO, Merck, Germany) and centrifuged for 2 min at 4700 rpm at 4 °C. Concentrated phages (100–200 μl) were further amplified and the concentration was measured using Nanodrop device following Smith's lab's protocol (www.biosci.missouri.edu/smithgp). The starting concentration of each phage solution before the next round of positive screening was set to $2–8x10^{12}$ vir/ml. Five rounds of positive screening were performed before obtaining the phages with high Cu(II) binding affinities.

In order to eliminate the virus binding to selected interfering M^+ metal ions (Al(III), Co(II), Cu(II), Fe(II), Ni(II) and Zn(II)), additional negative screening experiments were performed. Each negative screening was repeated by lowering the starting phage concentration to 10^{10}-10^{11} vir/ml until the virus binding was minimized according to ELISA test results.

2.2. DNA isolation and sequence analyses

After phage biopanning experiments, plaque formation assay was performed by following the manufacturer's instructions (Ph.D.-7 Phage display peptide library kit, NEB GmbH, Germany). 15 plaques were randomly selected, single stranded DNAs (ssDNAs) were isolated using QIAGEN plasmid isolation mini kit by applying an additional buffer (MP buffer) following the manufacturer's protocols (QIAprep M13 Handbook) and sent for sequencing (Eurofins Genomics, Germany).

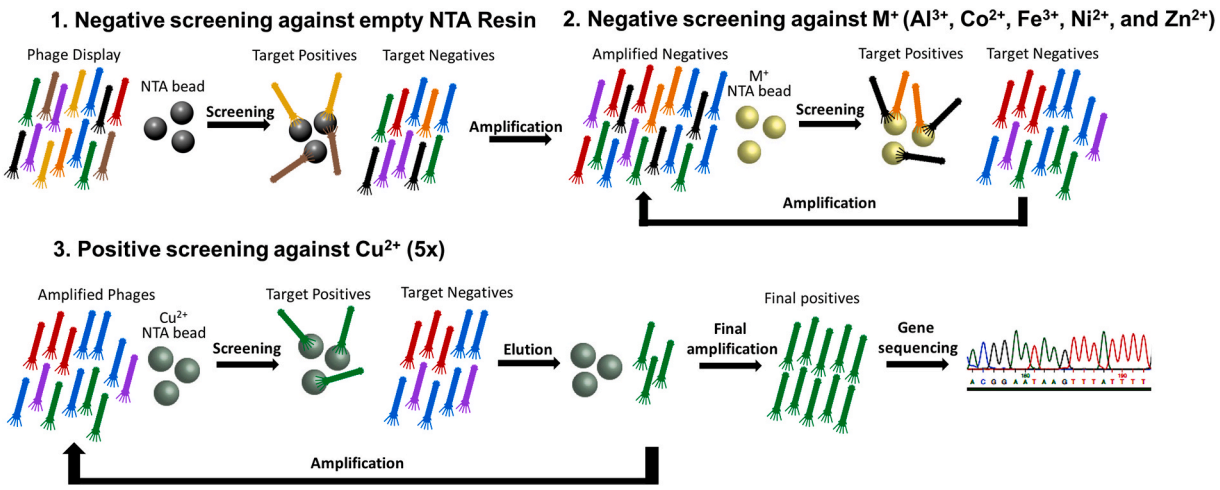

Fig. 1. Schematic work flow showing the phage biopanning steps conducted with agarose-based NTA beads.

2.3. Enzyme-linked immunosorbent assay (ELISA) tests

10 µl NTA MagBeads (Cube Biotech, Germany) functionalized with various metal ions (Al(III), Co(II), Cu(II), Fe(II), Ni(II) and Zn(II)) were washed and resuspended in 900 µl 1xPBS (pH 7.4) solution. 100 µl of phage solution (10^{11} vir/ml) was added and incubated on a rolling drum for 30 min at room temperature. Beads were washed with 1 ml PBS at least six times by vigorous vortexing and magnetic collection to remove loosely bound viruses. Washed beads were blocked in 1 ml 4% skim milk solution and incubated overnight at 4 °C on a rolling drum. After washing the beads three times with PBS, 1 ml of anti-M13-HRP (1:40000 in PBS, GE Healthcare, USA) was pipetted to each and incubated for 1 h by rolling at room temperature. After six times washing with 1 ml 0.5% Tween 20 solution by vigorous vortexing and magnetic collection, 200 µl of 3,3′,5,5′-tetramethylbenzidine (TMB) substrate solution (Sigma-Aldrich, USA) was added and incubated for 1 min before stopping the reaction with 200 µl of TMB stop reagent (Sigma-Aldrich, USA). 200 µl of supernatants was collected and the absorbance at 450 nm (620 nm reference) was measured using a microplate reader (SPECTRA Rainbow, TECAN, Switzerland).

2.4. Functionalization of cytopore beads with Cu-5 viruses

Cytopore microcarriers of 200–280 µm diameter (GE Healthcare, USA) were first hydrated in MilliQ at a final concentration of 10 mg/ml, autoclaved and functionalized with Cu-5 viruses following Yang et al. [20] with some modifications. After three times washing with MilliQ, 6 ml beads were mixed with 6 ml Cu-5 phages (10^{12} vir/ml in PBS) and incubated at 37 °C, 100 rpm overnight. Functionalized microcarriers were washed six times with MilliQ water using a 20 µm mesh sized filter (pluriSelect Life Science, Germany) to remove the unbound phages and resuspended in 6 ml MilliQ.

2.5. Colloidal coomassie staining and zeta potential measurements

Coomassie staining was performed as previously reported [24] and adapted for the cytopore beads. Briefly, 100 µl of cytopore microcarriers (with/without viruses) was mixed with 1 ml of Staining solution and incubated on an orbital shaker for 1 h at room temperature. Samples were first twice washed with MilliQ, destained and light microscopy images were taken.

Zeta potential of Cytopore beads before and after virus immobilization was analyzed using a Zetasizer Nano ZS ZEN3600 (Malvern Instruments Limited, UK). Disposable folded capillary cells (DTS1070) were filled with 1:100 MilliQ diluted bead samples and each measurement was run ten times. Three sets of measurements were performed for each sample.

2.6. ICP-MS measurements

The protocol used for evaluation of the binding adsorption efficiency of the prepared beads was adapted from previous study [30]. Analysis of all samples collected before and after contact with modified beads was performed on an iCAP q-ICP-MS (Thermo Fisher Scientific, Bremen, Germany), equipped with an auto sampler SC-E2 DX (Elemental Scientific, Omaha, USA). To perform the experiments, 2 µL liquid taken after contact with beads under static condition (24 h) was diluted in 50 mL of DI water supplemented with 2% HNO_3. The calibrators were prepared in the range from 200 ppt to 100 ppb. Cu_{63} isotope was monitored in a high-resolution mode to avoid any interference driving from the matrices and any interference possibly formed between the plasma gas and targeted elements. Prior to measurements, the instrument was tuned utilizing a standard polyelement tune-up solution (ELEMENT, Thermo Fisher Scientific, Bremen, Germany). All calibration solutions, blank and real samples were supplemented with 2% of HNO_3 prior to ICP-MS analysis. All measurements from the same batch were performed in triplicate and the final results were expressed as mean values with relative standard deviation. For data analysis QTEGRA software was used. The accuracy of quantification procedure was estimated by calculating the recoveries between the experimentally determined and expected (theoretical) concentration values. The accuracy of the ICP-MS method optimized for detection of Cu_{63} was ranged between 96% and 102%. As a blank, the same measurements with unmodified beads were conducted and their adsorption ability was evaluated.

2.7. AP-MALDI-MS study

2.7.1. Sample preparation

For analysis of interactions between the Cu-5 peptide (HGFANVA, synthetically synthesized by BioCat GmbH (Germany)) and Cu(II), 100 µl of 1 mM peptide solution was mixed with 500 µl of 1 mM Cu(II) solution and incubated on a rolling drum at room temperature for at least 1 h. Standard MALDI experiments were performed using the drying droplet method (1 µL) by mixing equal amounts of sample and CHCA matrix solution (5 mg/mL in 50:50 [v/v] in water/acetonitrile).

2.7.2. Mass spectrometry

AP-MALDI experiments were performed on a Bruker (Bremen, Germany) Esquire HCT+ 3D ion trap mass (IT) spectrometer fitted with a MassTech (Burtonsville, MD, USA) atmospheric pressure (AP)-MALDI

ion source and Nd:YAG solid-state laser (355 nm, 200 Hz) used in a spiral operation mode. Mass spectra were acquired in positive ion full-scan and MS/MS mode from *m/z* 300–1500 with a following source parameters: capillary voltage, −2500 V; end plate offset, −500 V; skimmer, 40.0 V; cap exit, 128.5 V; drying gas, 6.0 L/min; drying temperature, 120 °C.

2.8. Electron microscopy

Magnetic NTA beads collected after ELISA tests were investigated with FEI Quanta 250 FEG scanning electron microscope (FEI Company, USA) operated at 10 kV in high vacuum. Elemental composition analyses were performed using EDAX™ Team EDX system. Samples were immobilized on industrial scale standard Si wafers (5 × 5 mm) having a native oxide layer after cleaning in 1:1 mixture of isopropanol-acetone solution through sonication for 20 min at room temperature.

2.9. Preparation of AuNP-peptide system and Cu(II) sensing

A master reaction mixture for N number of samples (Nx100 µl of PBS stabilized AuNPs with a diameter of 20 nm (Sigma-Aldrich, USA)) was mixed with Nx20 µl of Cu-5 peptides (10 µM) tagged with three Cys units at C-terminal (HGFANVACCC referred as Cu-5_3Cys), synthetically synthesized by BioCat GmbH (Germany), was prepared. After 2 h incubation at room temperature on a rolling drum, 120 µL of AuNP-peptide complex was mixed with 100 µl of Cu(II) solution (0.1–10 µM), vortexed and incubated for an additional 30 min at room temperature on a rolling drum. UV–Vis spectroscopy measurements were performed between 400 nm and 700 nm wavelengths using a plate reader (TECAN, Switzerland). All measurements were conducted at least in triplicates and at least three independent experiments were performed. Negative control experiments were performed with Cu-5 peptides without any additional Cys units (HGFANVA) or without any peptide using only AuNPs following the same protocol.

A linear relationship was obtained between the concentration of Cu (II) ions and the absorbance ratio at 700 nm and 523 nm (Abs700/Abs523) of AuNP-peptide system upon Cu(II) treatment. The detection limit (LOD) was calculated according to Mei et al., 2015 [25] as LOD = 3σ/k where σ is the standard deviation of blank sample (with AuNPs and peptides but without any Cu(II) ions) after 5 measurements (n = 5) and k is the slope of the linear function between Cu(II) concentration versus Abs700/Abs523.

3. Results and discussion

3.1. Phage display selection and initial metal ion binding tests

In order to obtain specific peptide sequences which can selectively bind Cu(II) ions, phage display selection technique was applied by screening a library of M13 viruses against NTA beads functionalized with Cu(II) ions (Cu-NTA) and interfering metal ions of Al(III), Co(II), Fe (III), Ni(II) and Zn(II) (M^{+}-NTA). After collecting the viruses which do not bind bare NTA beads after negative screening, five positive screenings were performed against Cu-NTA beads. Negative screenings were repeated several times by considering the ELISA test results performed after each round of screening to confirm the selectivity of the enriched phage library against Cu(II) ions. ELISA results obtained with the final phage library solution after all positive and negative screenings are shown in Fig. 2a. The strongest binding affinity was observed against Cu (II). Magnetic NTA beads were next investigated by SEM analyses. EDX measurements revealed the typical C, O and Fe peaks in all samples confirming the presence of cross-linked agarose and magnetic particles

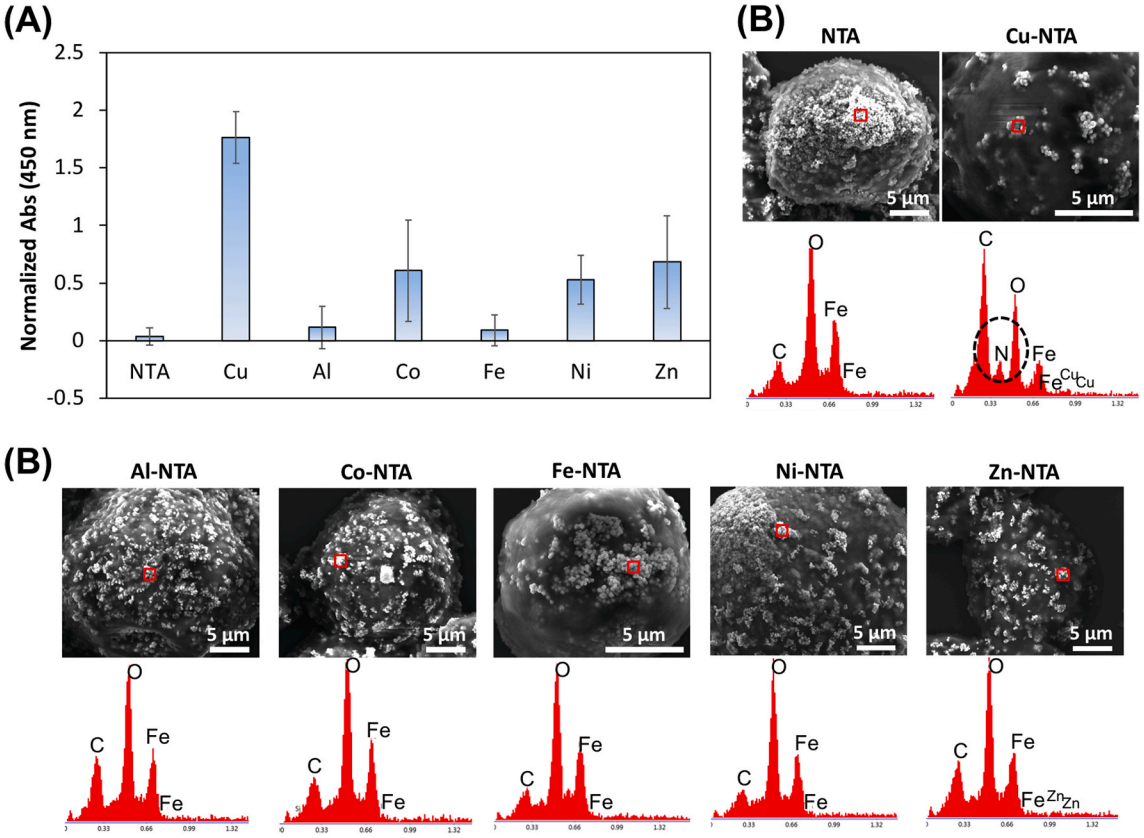

Fig. 2. Metal ion binding affinity tests with final Cu(II) binding phages after completing all negative/positive screenings. ELISA analyses (A) were conducted with metal ion coated magnetic NTA beads which were later investigated by SEM imaging (B). SEM analyses were conducted at 10 kV at high vacuum. EDX spectra were taken inside the red boxes. (For interpretation of the references to color in this figure legend, the reader is referred to the Web version of this article.)

which are the main constituents of spherical magnetic NTA beads (Fig. 2b). Whilst magnetic particles were observed as brighter spots, remaining bead surfaces were detected as darker areas implying the presence of some organic material which should be phages and agarose. Most interestingly, magnetic Cu-NTA beads were observed to be covered with a much darker layer where only a few bright spots of magnetic particles were seen. EDX analyses conducted on Cu-NTA beads showed a strong N peak which hints at the presence of phage organic material. Rest of the beads did not show strong N signal implying that most of the phages were immobilized on Cu-NTA beads which is in line with the ELISA results.

3.2. Identification of Cu(II) binding peptides

After completing the phage screening experiments, 15 monoclonal M13 virus plaques were randomly selected, ssDNAs were isolated and sent for sequencing analyses. 14 of the clones were successfully sequenced and 3 different peptide sequences with various frequencies of occurrence were obtained as listed in Table 1. One of the peptides, referred as "Cu-5 peptide" with the sequence HGFANVA, showed the highest frequency of occurrence making it a good Cu(II) binding peptide candidate. Although the peptide #11 was observed four times, it was not considered due to the included stop codon. The third candidate peptide with the sequence HNAPTH was named as "Cu-14 peptide", which occurred three times. The common characteristic of the obtained peptide sequences is the presence of nonpolar amino acids at the first glance which is in line with Cr(III) binding peptide sequences reported by Yang et al., 2015 [20]. It was stated that nonpolar amino acids might take role in folding of the peptides to form favorable 3D confirmations for specific Cr(III) binding implying that these nonpolar units could also help for Cu (II) ion binding. The next common feature of all three peptides is that they are rich in N- containing functional groups (-NH_2, –NH) which has been also observed by Yang et al., 2018 [21] for their newly identified As (III) binding peptides where they discussed that the N- containing functional groups can bind metals through coordination. In order to form a complex with a metal ion, there should be either an amide nitrogen or a carbonyl oxygen available in the peptide backbone [26,27] which are both present in all of the three candidate peptide sequences most probably favoring the Cu(II) ion binding. Moreover, all peptide sequences have histidine (H) units, which are well known for their metal ion complexation properties and very often used as a protein tag in biotechnology studies especially for recombinant protein purification applications [28].

3.3. Cu(II) specificity tests of the selected phages and AP-MALDI-MS analysis of selected peptides

Metal ion binding affinities of two candidate peptides, Cu-5 and Cu-14, were further investigated by ELISA analyses. Both Cu-5 and Cu-14 phages showed considerably stronger binding affinities to Cu-NTA beads than the other M^+-NTA beads (Fig. 3) which is in accordance with the ELISA measurements conducted with the final phage libraries before sequencing analyses (Fig. 2). Interestingly, Cu-14 phages were

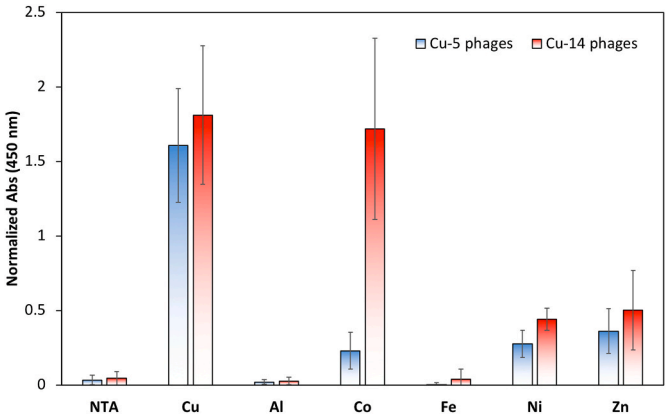

Fig. 3. Metal ion binding selectivity tests with Cu-5 and Cu-14 phages through ELISA analyses.

observed to bind Co-NTA beads as strong as Cu-NTA beads although Cu-5 phages did not show significant affinity to Co-NTA beads. Thus, Cu-5 phages were selected as Cu(II) specific viruses.

Cu-5 peptides (HGFANVA) were synthetically synthesized and mass-spectrometry analysis was performed in order to verify the interaction between Cu(II) ions and peptide molecules. Fig. 4 shows MALDI-MS spectra of a mixture of Cu-5 peptide and Cu(II) solution. The recorded mass spectra (in position detection mode) exhibited by protonated species are corresponding to the intact peptide at *m/z* 715.5 and clusters at *m/z* 777 and 779 arising from the Cu_{63} and Cu_{65} isotopes. This indicates that the binding between the targeted peptide and Cu(II) can be readily described by a 1:1 model.

3.4. Virus immobilization on cytopore beads and initial Cu(II) binding tests

In order to confirm the specific Cu(II) ion binding of Cu-5 viruses from liquid samples, a host system was constructed using positively charged cytopore beads. A suitable host material was necessary since M13 viruses alone are highly dispersed in liquid solutions making them difficult to isolate by means of classical laboratory tools like high-speed centrifugation [20]. Zeta potential measurements showed that cytopore beads were positively charged under physiological conditions (Fig. 5c). Therefore, negatively charged M13 viruses were easily adsorbed on cytopore beads through electrostatic interactions. Zeta potential of functionalized cytopore beads dropped to ca. −5 mV implying that virus loading was successful (Fig. 4c). Moreover, Coomassie staining resulted in typical blue coloring of the cytopore beads after virus treatment confirming the viral attachment (Fig. 5a-b).

Next, cytopore beads functionalized with Cu-5 viruses and the bare beads alone as negative control were incubated with various concentrations of Cu(II) solutions (3.14, 6.68 and 21.90 μg/L). Supernatants were collected and Cu(II) concentrations were determined by ICP-MS measurements. Calculated sorption efficiencies are seen in Fig. 5d. Although the bare beads did not bind significant amounts of Cu(II) ions

Table 1
Sequence information of identified Cu(II) binding candidate peptides, their frequency of occurrence, corresponding amino acid properties and number of N-, S-, –OH and –COOH containing functional groups in their side chains.

No.	DNA sequence	Peptide sequence	Frequency	Properties[a]	N[b]	S[b]	-OH[b]	-COOH[b]
5	catgggtttgcgaatttgct	HGFANVA	7/14	bnnnpnn	3	–	–	1
11	gcgcatttgtagagtgttttg	AHL-SVL	4/14	nbn-onn	2	–	1	1
14	cataatgctcctactaatcat	HNAPTH	3/14	bpnnopb	6	–	1	2

-OH group containing (o) amino acids are S, T and Y. Acidic and polar (a) amino acids are D and E. Basic and polar (b) amino acids are K, R and H.
[a] Nonpolar amino acids (n) are A, V, L, I, F, W, M, P and G. Polar and uncharged (p) amino acids are C, N and Q.
[b] N- containing functional groups are found in side chains of H (2 N atoms), K, N, P, Q, R (3 N atoms) and W. S- containing functional groups are found in C and M. –OH containing side groups are seen in S, T and Y. –COOH containing side chains are found in D,E and P.

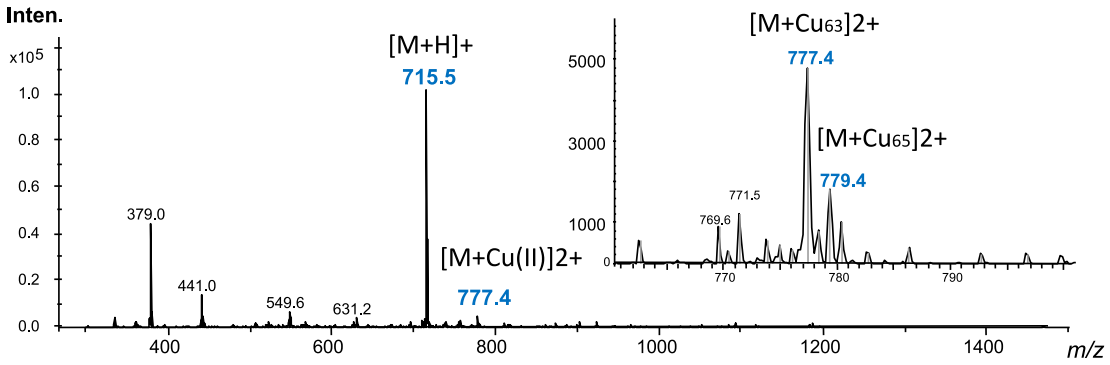

Fig. 4. AP-MALDI-MS full scan recorded for targeted Cu-5 peptide (HGHAVA) after adsorption of 1 mM Cu(II) (as a case study). Inset shows the zoomed in mass spectra corresponding to peptide-Cu(II) clusters. *Note:* due to dilution with CHCA the current spectrum corresponds to 500 µM of Cu(II); laser fluence 45%.

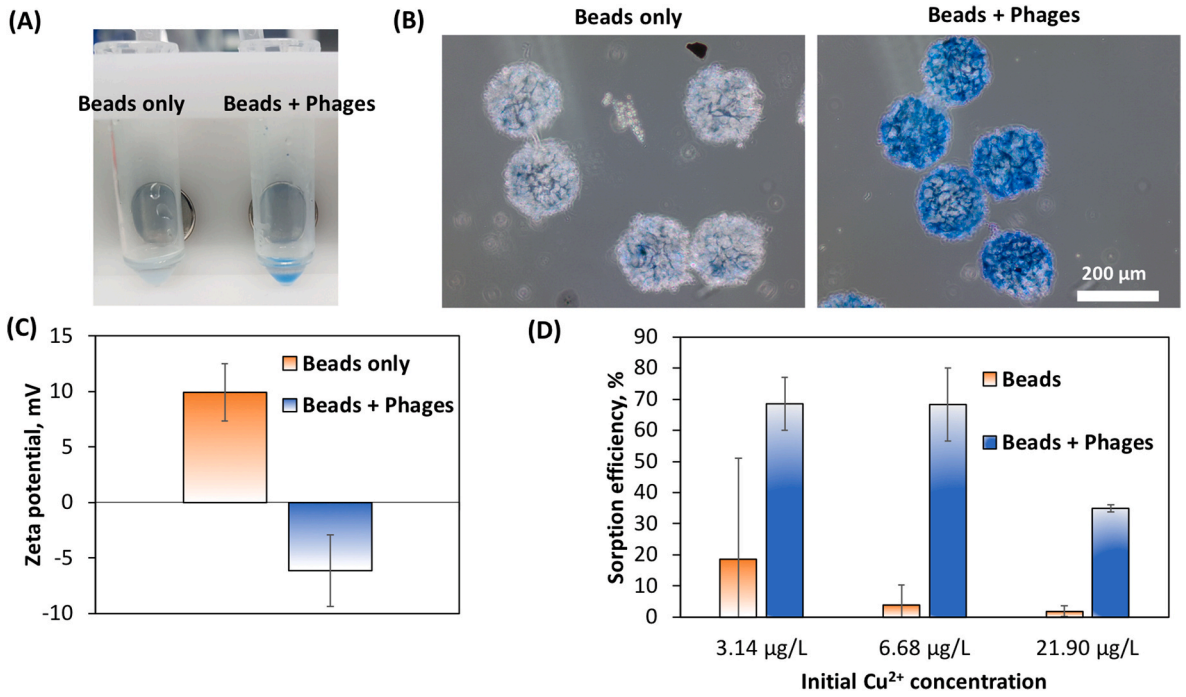

Fig. 5. Digital camera (A) and light microscopy (B) images of cytopore beads without and with Cu-5 viruses after colloidal Coomassie staining. (C) Zeta potential analyses of cytopore beads before and after immobilization of Cu-5 phages. (D) Sorption efficiencies of cytopore beads with/without Cu-5 phages treated with various concentrations of Cu(II) solutions. Starting and end concentrations of Cu(II) ions were quantified by ICP-MS.

(sorption efficiencies < 20%), Cu-5 virus activated cytopore beads were observed to adsorb significant amounts of Cu(II) ions (around 70% sorption efficiency when treated with 6.68 µg/L Cu^{2+}). As the Cu(II) concentration was elevated to 21.90 µg/L, virus functionalized beads were observed to be saturated with Cu (II) ions resulting in lower sorption efficiencies which was around 35%.

3.5. Cu(II) sensing with synthetically synthesized Cu-5 peptides tagged with cys units

The Au–S binding is one of the most common interaction methods applied for functionalization of Au surfaces with biological molecules for various applications ranging from medicine to biosensor related studies [29]. For example, Chen et al., 2014 [31] incorporated an N-terminal tag including one Cys unit (CGGG) to a pre-reported Cu(II) binding peptide modified from a coiled-coil peptide (Wang et al., 2012 [32]) to induce AuNP binding through Au–S covalent bond formation. In this study, in order to trigger selective Au binding and at the same time Cu(II) attachment as a bifunctional manner, Cu-5 peptides were synthetically synthesized with three additional Cys units (designated as Cu-5_3Cys) at C- terminal (Fig. 6a). Au binding affinities of engineered Cu-5_3Cys peptides were investigated by incubating various concentrations of peptide solutions with PBS stabilized AuNPs (diameter of 20 nm). AuNPs showed a surface plasmon resonance (SPR) peak at around 523 nm in the absence of peptides and this peak was conserved until a peptide concentration of 10 µM implying that the peptide binding through Au–S interaction did not disturb the dispersity of AuNPs (Fig. 6b).

Synthetically synthesized Cu-5_3Cys peptide molecules were shown to stably bind AuNPs without causing any aggregation at a peptide concentration of 10 µM. This AuNP-peptide complex was next incubated with Cu(II) solutions of varying concentrations (0, 0.1, 0.2, 0.5, 1, 2, 4, 6, 8 and 10 µM). It was expected that the Cu-5 peptides would specifically bind Cu(II) ions acting as a bridge between AuNP-peptide complexes causing aggregation (Fig. 6a). UV–Vis absorption spectroscopy measurements showed the aggregation behavior of AuNPs and its dependency on Cu(II) concentration (Fig. 7a). As the Cu(II) concentration was decreased, absorbance intensities at 523 nm, which is the original

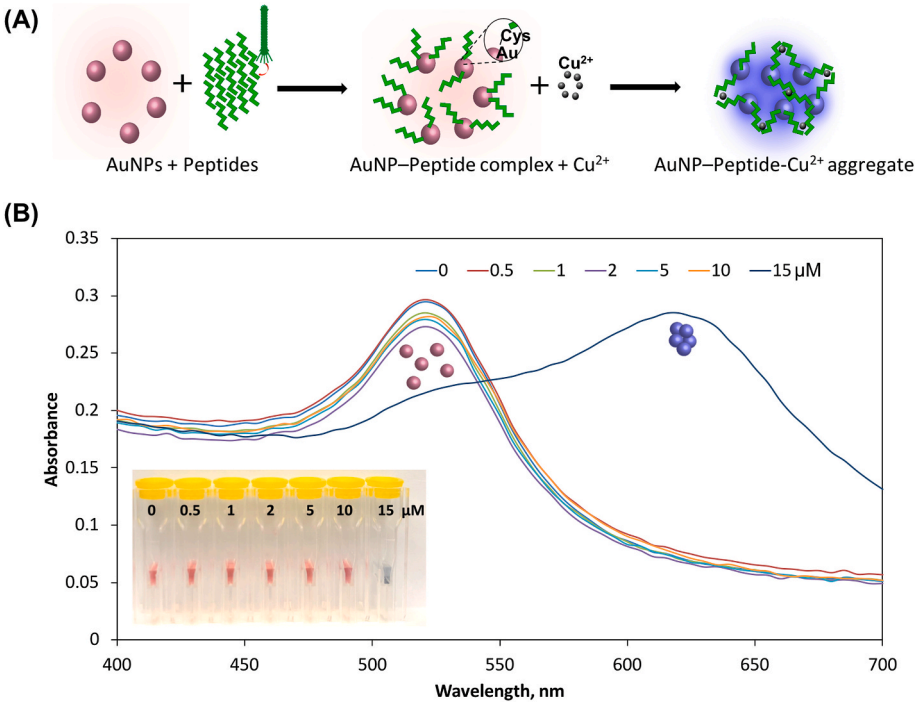

Fig. 6. Schematic drawing showing the interaction of AuNPs with Cu-5_3Cys peptides and the expected aggregation behavior after Cu(II) treatment (A). 20 nm PBS stabilized AuNPs were incubated with various concentrations of peptide solutions and monitored through UV–Vis absorption spectroscopy analyses (B). Inset image shows the corresponding digital camera image of the reaction mixtures.

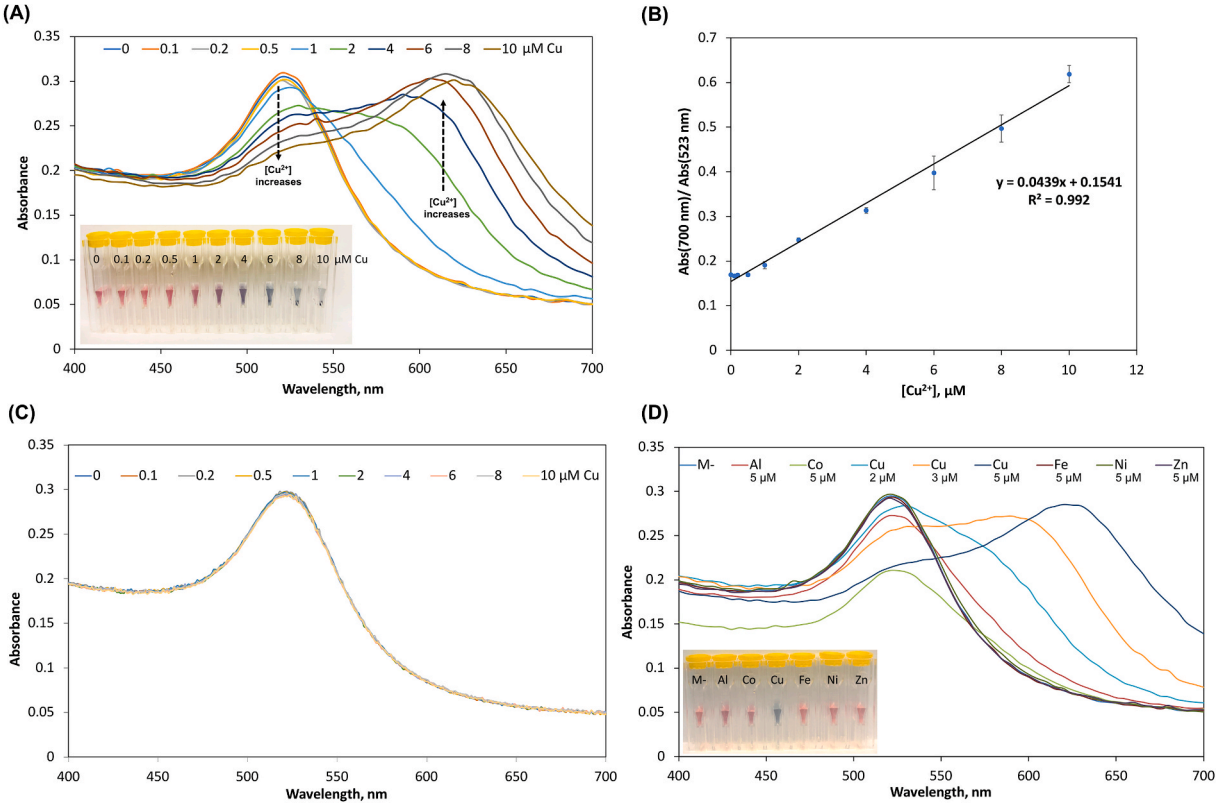

Fig. 7. (A) UV–Vis absorption spectra of Cu-5_3Cys (HGFANVACCC) peptide functionalized 20 nm AuNPs treated with various concentrations of Cu(II) (0, 0.1, 0.2, 0.5, 1, 2, 4, 6, 8 and 10 µM). The inset shows the color change of the reaction mixture with varying Cu(II) concentrations. (B) Response of colorimetric assay system in terms of absorbance ratios at 700 and 523 nm (Abs700/Abs523) versus Cu(II) concentration. (C) UV–Vis absorption spectra of AuNPs treated with Cu-5 (HGFANVA) peptides without any Cys units at various Cu(II) concentrations (0, 0.1, 0.2, 0.5, 1, 2, 4, 6, 8 and 10 µM). (D) Selectivity tests of the designed colorimetric system with various interfering metal ions (Al(III), Co(II), Fe(III), Ni(II) and Zn(II) at 5 µM and with Cu(II) at 2 µM, 3 µM and 5 µM as a control. Insets are the digital camera images of the samples. (For interpretation of the references to color in this figure legend, the reader is referred to the Web version of this article.)

SPR peak position of AuNPs, were observed to drop (Fig. 7a). Moreover, broadening and right shifting of the absorption spectra were seen at elevated Cu(II) concentrations showing that the AuNPs were not dispersed anymore. A clear color change from red to blue was observed which could easily be detected by naked eye (Fig. 7a-inset). On the contrary, control experiments conducted with Cu-5 peptides (HGFANVA) without any additional Cys units did not cause any AuNP aggregation upon incubation with Cu(II) solutions of varying concentrations (0, 0.1, 0.2, 0.5, 1, 2, 4, 6, 8 and 10 μM) confirming the AuNP binding role of Cys units (Fig. 7c). In the designed peptide structure, while HGFANVA sequence serves as the Cu(II) binding domain, 3xCys tag triggers AuNP binding. Similarly, no aggregation was observed upon incubation of Cu(II) solutions with only AuNPs (data not shown). Since the decrease in absorbance values at 523 nm and the right shift of the SPR spectra together with the increase in absorption intensities at 700 nm seem to be related to applied Cu(II) concentration, the ratio of absorbance intensities at 700 nm and 523 nm (Abs700/Abs523) was expected to reflect the degree of AuNP aggregation which could be plotted against Cu(II) concentration. Indeed, Abs700/Abs523 was linearly proportional to Cu(II) concentration with an R^2 value of 0.992 (Fig. 7b). The limit of detection (LOD) of the case study shown in Fig. 6 was calculated to be 91.15 nM (3σ/k, n = 5, ca. 5.8×10^{-3} mg/L). Moreover, the average LOD of three independent experiments was estimated to be 97.31 ± 14.11 nM (3σ/k, n = 5) which is much lower than the World Health Organization (WHO)'s guideline of 1.3 mg/L [4] implying that this system could be used for on-site detection of Cu(II) ions from environmental samples.

A similar colorimetric Cu(II) ion sensing approach was reported by Chen et al., 2014 [31] using a pre-identified Cu(II) binding peptide (SIRKLEYEIEELRLRIG) modified from a coiled-coil peptide (Wang et al., 2012 [32]). In our study, we performed a wet-lab approach for identifying Cu(II) specific peptides using phage libraries ending up with a heptapeptide sequence (HGFANVA) which is much shorter than the 17 amino acid long SIRKLEYEIEELRLRIG peptide. Chen et al., inserted an N-terminal tag including one Cys unit (CGGG) to their construct obtaining a 21 amino acid long peptide (CGGG SIRKLEYEIEELRLRIG) to induce AuNP binding through Au–S covalent bond formation and obtained a Cu(II) detection limit of 1 μM. Moreover, Chang et al., 2017 [33] triggered AuNP aggregation by electrostatic interactions between ammonium cations of cysteamine molecules, citrate capped AuNPs and Cu(II) ions reporting a Cu(II) detection limit of 1.52 μM. In the current study, AuNP binding of Cu-5 peptides was mediated through a 3xCys (CCC) tag at C-terminal of the HGFANVA peptide resulting in a decapeptide (10 amino acid units, HGFANVACCC) achieving an average LOD of 97.31 ± 14.11 nM.

The selectivity of AuNP-peptide complex system was next tested with the candidate interfering metal ions (Al(III), Co(II), Fe(III), Ni(II) and Zn(II)) by replacing Cu(II) in the optimized sensor system. No significant absorbance spectra or color change was observed as a response with the interfering metal ions implying that the AuNP-peptide complex was selective for Cu(II) ions (Fig. 7d) which can operate as a colorimetric detection system (Fig. 7a & b).

4. Conclusion

In this study, highly selective Cu(II) binding peptides were identified through genuine phage display technique after five rounds of positive screening. Following various rounds of negative screening performed against competitive metal ions (Al(III), Co(II), Fe(III), Ni(II) and Zn(II)), bacteriophages were eluted and enriched. Enzyme Linked Immunosorbent Assay (ELISA), Scanning Electron Microscopy (SEM) and Energy Dispersive X-ray spectroscopy (EDX) analyses confirmed the selective Cu(II) binding of final phage libraries. Gene sequencing analyses of 15 randomly selected phage clones resulted in three different candidate peptide sequences. The highest frequency of occurrence and the strongest Cu(II) affinity was observed with Cu-5 peptide, which was therefore chosen for further Cu(II) detection and removal tests. Selective Cu(II) binding of engineered viruses was demonstrated by Inductively Coupled Plasma-Mass Spectrometry (ICP-MS). Mass spectrometry analyses suggested that Cu-5 peptide molecules bind Cu(II) ions following a 1:1 model. A colorimetric Cu(II) detection system was validated with synthetically synthesized Cu-5 peptides tagged with Cys units at C-terminal and AuNPs. The "AuNP-peptide complex" based Cu(II) sensing was highly selective against Cu(II) and the limit of detection (LOD) was calculated as 91.15 nM (3σ/k, n = 5, ca. 5.8×10^{-3} mg/L) for the case study which is much lower than the World Health Organization (WHO)'s guideline of 1.3 mg/L [4] implying that this biosensor could be used for on-site detection of Cu(II) ions from environmental samples. The interdisciplinary approach of this study implies that it is possible to design biosensors in the future with improved selectivity and sensitivity which are portable, simple and cost-effective. It is important to note that for future phage display selection studies, a wider range of competing metal ions including Cd(II) and As(III) could be applied in order to further increase the selectivity of discovered peptides. Moreover, as a future work, it would be interesting to investigate the Cu(II) binding affinities of cropped peptide fragments (i.e. HGF, HGFA, etc.) in order to study the effect of each amino acid residue on Cu(II) binding.

Funding

Korea Institute of Science and Technology-Europe basic research program (11906 & 12006).

Ethical approval

This article does not contain any studies with human participants or animals performed by any of the authors.

Informed consent

Informed consent was obtained from all individual participants included in the study.

Credit author statement

Nuriye Korkmaz: Conceptualization, Methodology, Investigation, Validation, Writing - original draft - review & editing, Visualization, Project administration, Funding acquisition. Changhyun Hwang: Investigation, Validation, Visualization, Writing - original draft. Kim Kristin Kessler: Investigation, Validation, Visualization. Yuliya E. Silina: Investigation, Validation, Visualization, Writing - review & editing. Lisann Müller: Investigation, Validation. Jayoung Park: Investigation, Validation.

Declaration of competing interest

The authors declare that they have no known competing financial interests or personal relationships that could have appeared to influence the work reported in this paper.

Acknowledgements

This work was supported by Korea Institute of Science and Technology Europe Forschungsgesellschaft mbH (Saarbrücken, Germany) Basic Research Fund (11906 & 12006).

References

[1] H. Ali, E. Khan, I. Ilahi, Environmental chemistry and ecotoxicology of hazardous heavy metals: environmental persistence, toxicity, and bioaccumulation, J. Chem. https://doi.org/10.1155/2019/6730305.

[2] M.A. Ashaiekh, M.A. Eltayeb, A.H. Ali, A.M. Ebrahim, I. Salih, A.M. Idris, Spatial distribution of total and bioavailable heavy metal contents in soil from agricultural,

residential, and industrial areas in Sudan, Toxin Rev. 38 (2019) 93–105, https://doi.org/10.1080/15569543.2017.1419491.
[3] G. L. Turdean, Design and development of biosensors for the detection of heavy metal toxicity, Int. J. Electrochem. https://doi.org/10.4061/2011/343125.
[4] M.B. Gumpu, S. Sethuraman, U.M. Krishnan, J.B.B. Rayappan, A review on detection of heavy metal ions in water–an electrochemical approach, Sensor. Actuator. B Chem. 213 (2015) 515–533, https://doi.org/10.1016/j.snb.2015.02.122.
[5] E.S. Forzani, H. Zhang, W. Chen, N. Tao, Detection of heavy metal ions in drinking water using a high-resolution differential surface plasmon resonance sensor, Environ. Sci. Technol. 39 (2005) 1257–1262, https://doi.org/10.1021/es049234z.
[6] K. Dutta, S. Panda, Identification of the levels of interference of ions toward heavy metal detection in electrochemical sensors using the barrier width technique, J. Electrochem. Soc. 165 (2018) B378–B389, https://doi.org/10.1149/2.1331809jes.
[7] X. Han, C. Li, D. Yong, Microbial electrode sensor for heavy-metal ions, Sensor. Mater. 31 (2019) 4103–4111, https://doi.org/10.18494/SAM.2019.2645.
[8] A. Sarkar, K.D. Sarkar, V. Amrutha, K. Dutta, An overview of enzyme-based biosensors for environmental monitoring, in: S.K. Brar, K. Hegde, V.L. Pachapur (Eds.), Tools, Techniques and Protocols for Monitoring Environmental Contaminants, Elsevier, 2019, pp. 307–329, https://doi.org/10.1016/B978-0-12-814679-8.00015-7.
[9] M. Bilal, H.M. Iqbal, Microbial-derived biosensors for monitoring environmental contaminants: recent advances and future outlook, Process Saf. Environ. 124 (2019) 8–17, https://doi.org/10.1016/j.psep.2019.01.032.
[10] N. Joshi, X. Wang, L. Montgomery, A. Elfick, C.E. French, Novel approaches to biosensors for detection of arsenic in drinking water, Desalination 248 (2009) 517–523, https://doi.org/10.1016/j.desal.2008.05.096.
[11] J. Ma, M.K. Sengupta, D. Yuan, P.K. Dasgupta, Speciation and detection of arsenic in aqueous samples: a review of recent progress in non-atomic spectrometric methods, Anal. Chim. Acta 831 (2014) 1–23, https://doi.org/10.1016/j.aca.2014.04.029.
[12] T.T. Ngo-Duc, Z. Alibay, J.M. Plank, J.E. Cheeney, E.D. Haberer, Gold-decorated M13 I-forms and S-forms for targeted photothermal lysis of bacteria, ACS Appl. Mater. Interfaces 12 (2019) 126–134, https://doi.org/10.1021/acsami.9b15682.
[13] G.P. Smith, Phage display: simple evolution in a petri dish (nobel lecture), Angew. Chem. Int. Ed. 58 (2019) 14428–14437, https://doi.org/10.1002/anie.201908308.
[14] F. You, G. Yin, X. Pu, Y. Li, Y. Hu, Z. Huang, X. Liao, Y. Yao, X. Chen, Biopanning and characterization of peptides with Fe3O4 nanoparticles-binding capability via phage display random peptide library technique, Colloids Surf. B Biointerfaces 141 (2016) 537–545, https://doi.org/10.1016/j.colsurfb.2016.01.062.
[15] P. Hou, G. Zhao, C. He, H. Wang, H. He, Biopanning of polypeptides binding to bovine ephemeral fever virus G 1 protein from phage display peptide library, BMC Vet. Res. 14 (2018) 1–9, https://doi.org/10.1186/s12917-017-1315-x.
[16] D. Ferreira, A.P. Silva, F.L. Nobrega, I.M. Martins, C. Barbosa-Matos, S. Granja, S. F. Martins, F. Baltazar, L.R. Rodrigues, Rational identification of a colorectal cancer targeting peptide through phage display, Sci. Rep. 9 (2019) 1–12, https://doi.org/10.1038/s41598-019-40562-1.
[17] J.W. Day, C.H. Kim, V.V. Smider, P.G. Schultz, Identification of metal ion binding peptides containing unnatural amino acids by phage display, Bioorg. Med. Chem. Lett 23 (2013) 2598–2600, https://doi.org/10.1016/j.bmcl.2013.02.106.
[18] M. Mejare, S. Ljung, L. Bülow, Selection of cadmium specific hexapeptides and their expression as OmpA fusion proteins in Escherichia coli, Protein Eng. Des. Sel. 11 (1998) 489–494, https://doi.org/10.1093/protein/11.6.489.
[19] R. Nian, D.S. Kim, T. Nguyen, L. Tan, C.W. Kim, I.K. Yoo, W.S. Choe, Chromatographic biopanning for the selection of peptides with high specificity to Pb2+ from phage displayed peptide library, J. Chromatogr. A 1217 (2010) 5940–5949, https://doi.org/10.1016/j.chroma.2010.07.048.
[20] T. Yang, X.Y. Zhang, X.X. Zhang, M.L. Chen, J.H. Wang, Chromium (III) binding phage screening for the selective adsorption of Cr (III) and chromium speciation, ACS Appl. Mater. Interfaces 7 (2015) 21287–21294, https://doi.org/10.1021/acsami.5b05606.
[21] T. Yang, X.X. Zhang, J.Y. Yang, Y.T. Wang, M.L. Chen, Screening arsenic (III)-binding peptide for colorimetric detection of arsenic (III) based on the peptide induced aggregation of gold nanoparticles, Talanta 177 (2018) 212–216, https://doi.org/10.1016/j.talanta.2017.07.005.
[22] F. Amourizi, K. Dashtian, M. Ghaedi, Electrostatically controlled plasmonic effects of gold nanoparticles with indigo-carmine functionation for rapid and straightforward colorimetric detection of Cu(II) ions, Spectrochim. Acta Mol. Biomol. Spectrosc. 230 (2020) 118026, https://doi.org/10.1016/j.saa.2020.118026.
[23] M.E. Letelier, M. Faúndez, J. Jara-Sandoval, A. Molina-Berríos, J. Cortés-Troncoso, P. Aracena-Parks, R. Marín-Catalán, Mechanisms underlying the inhibition of the cytochrome P450 system by copper ions, J. Appl. Toxicol. 29 (2009) 695–702, https://doi.org/10.1002/jat.1460.
[24] N. Dyballa, S. Metzger, Fast and sensitive colloidal coomassie G-250 staining for proteins in polyacrylamide gels, J. Vis. Exp. 30 (2009) e1431, https://doi.org/10.3791/1431.
[25] Q. Mei, Y. Shi, Q. Hua, B. Tong, Phosphorescent chemosensor for Hg 2+ based on an iridium (iii) complex coordinated with 4-phenylquinazoline and carbazole dithiocarbamate, RSC Adv. 5 (2015) 74924–74931, https://doi.org/10.1039/C5RA09609J.
[26] H. Sigel, R.B. Martin, Coordinating properties of the amide bond. Stability and structure of metal ion complexes of peptides and related ligands, Chem. Rev. 82 (1982) 385–426, https://doi.org/10.1021/cr00050a003.
[27] H. Kozłowski, W. Bal, M. Dyba, T. Kowalik-Jankowska, Specific structure–stability relations in metallopeptides, Coord. Chem. Rev. 184 (1999) 319–346, https://doi.org/10.1016/S0010-8545(98)00261-6.
[28] D. Brasili, J. Watly, E. Simonovsky, R. Guerrini, N.A. Barbosa, R. Wieczorek, M. Remelli, H. Kozlowski, Y. Miller, The unusual metal ion binding ability of histidyl tags and their mutated derivatives, Dalton Trans. 45 (2016) 5629–5639, https://doi.org/10.1039/C5DT04747A.
[29] D. Wu, Z. Zhang, Synergistic bio-recognition/spatial-confinement for effective capture and sensitive photoelectrochemical detection of MCF-7 cells, Chem. Commun. 55 (2019) 14514–14517, https://doi.org/10.1039/C9CC08521A.
[30] Y.E. Silina, M. Koch, P. Herbeck-Engel, C. Fink-Straube, Multi-dimensional hydroxyapatite microspheres as a filling material of minicolumns for effective removal at trace level of noble and non-noble metals from aqueous solutions, J. Environ. Chem. Eng. 6 (2018) 1886–1897, https://doi.org/10.1016/j.jece.2018.02.044.
[31] H. Chen, J. Zhang, X. Liu, Y. Gao, Z. Ye, G. Li, Colorimetric copper (II) ion sensor based on the conformational change of peptide immobilized onto the surface of gold nanoparticles, Anal. Methods. 6 (2014) 2580–2585, https://doi.org/10.1039/C3AY42211A.
[32] X. Wang, I. Bergenfeld, P.S. Arora, J.W. Canary, Reversible redox reconfiguration of secondary structures in a designed peptide, Angew Chem. Int. Ed. Engl. 51 (2012) 12099–12101, https://doi.org/10.1002/anie.201206009.
[33] C.C. Chang, C.H. Lee, T.H. Wu, C.P. Chen, C.Y. Chen, C.W. Lin, Reversion of gold nanoparticle aggregates for the detection of Cu 2+ and its application in immunoassays, Analyst 142 (2017) 4684–4690, https://doi.org/10.1039/C7AN01511A.
[34] P. Gonzalez, K. Bossak, E. Stefaniak, C. Hureau, L. Raibauta, W. Balc, P. Faller, N-terminal Cu binding motifs Xxx-Zzz-His (ATCUN) and Xxx-His and their derivatives: chemistry, biology and medicinal applications, Chem. Eur J. 24 (2018) 8029–8041, https://doi.org/10.1002/chem.201705398.
[35] A. Spriestersbach, J. Kubicek, F. Schäfer, H. Block, B. Maertens, Purification of his-tagged proteins, Methods Enzymol. 559 (2015) 1–15, https://doi.org/10.1016/bs.mie.2014.11.003.